

# Performance Variability of Polycrystalline Photovoltaic Modules under Monthly Climatic Fluctuations in Calabar, Nigeria

Julie C. Ogbulezie,<sup>1</sup> Samuel Chukwujindu Nwokolo,<sup>2,\*</sup> and Armstrong O. Njok<sup>3,\*</sup>

1: Department of Physics, Faculty of Physical Sciences, University of Calabar, Calabar, 540242, Nigeria

2: Atmospheric Physics/Meteorology Programme, Department of Physics, Faculty of Physical Sciences, University of Calabar, Calabar, Nigeria

3: Department of Physics, Faculty of Physical Sciences, University of Cross River State Calabar, Calabar, 540252, Nigeria

Received September 15, 2025; Accepted October 15, 2025; Published November 9, 2025

This study presents a high-resolution, in-situ analysis of the monthly performance of a domestic polycrystalline photovoltaic (PV) module operating within Calabar's humid monsoon climate, translating empirical field observations into practical design thresholds for residential applications and system installers. Using a digital plane-of-array solar irradiance meter in conjunction with an intelligent MPPT tracker, voltage, current, and power were monitored at 30-minute intervals between 06:00 and 18:00 from July to September. The analysis reveals a stable voltage plateau once plane-of-array solar irradiance exceeds approximately  $200 \text{ W m}^{-2}$ , corresponding to near-standard test condition (STC) voltages across all months. In contrast, achieving manufacturer-rated current during August–September would require irradiance levels exceeding  $1000 \text{ W m}^{-2}$ , which are seldom observed under real outdoor conditions. July exhibited the highest output current and power, while September recorded the lowest, despite August having the fewest sunshine hours. Notably, output power remained approximately uniform across the  $0\text{--}450 \text{ W m}^{-2}$  irradiance range, irrespective of month. At irradiance levels above approximately  $400 \text{ W m}^{-2}$ , conversion efficiency follows the order July > August > September, with the module's rated maximum power appearing unattainable in September under the observed operating conditions.

Significance/Novelty: (i) Provides location-specific, month-resolved operating thresholds ( $\geq 200 \text{ W m}^{-2}$  for voltage stability;  $>1000 \text{ W m}^{-2}$  required to approach rated current in wetter months), bridging the gap between laboratory specifications and real-world tropical performance; (ii) identifies counterintuitive seasonal behavior, wherein greater sunshine duration does not necessarily yield higher output, thereby informing climate-responsive sizing of storage and inverter systems; and (iii) establishes actionable heuristics—uniform power response under low-to-moderate irradiance and month-dependent efficiency—that reduce performance uncertainty, mitigate premature system abandonment, and promote reliable PV deployment for energy access and net-zero transitions in southern Nigeria.

*Keywords: Solar irradiance (plane-of-array); Month; Polycrystalline PV module; Maximum power point; Efficiency*

## Introduction

Renewable energy is an inexhaustible resource that is clean, quiet, and minimally polluting. Photovoltaic technology represents one of the most efficient and accessible means of electricity generation, offering a low-maintenance solution powered by a free and abundant energy source available in many countries [1]. Photovoltaic technology enables electricity generation with minimal technical expertise, as users are primarily required to install the modules in unobstructed areas and maintain clean, dust-free surfaces for optimal performance [2].

It is well established that fossil fuel reserves are finite [3], and their continued use poses severe environmental risks. The combustion of fossil fuels significantly contributes to climate change, global warming, air pollution, and acid rain, underscoring the urgency of transitioning to sustainable energy sources [4-6]. Therefore, there is an urgent need to advance renewable energy technologies to address the political, economic, and environmental challenges associated with electricity generation [7]. It is therefore essential to evaluate the most suitable renewable options for specific locations to reduce the global carbon footprint. The anticipated depletion of fossil fuel reserves has further accelerated technological progress in the renewable energy sector, particularly in photovoltaics [8].

The Russia–Ukraine conflict has resulted in a significant global shortage of fossil fuel products, leading to unprecedented price increases [9]. Despite Nigeria's position as a major fossil fuel exporter, domestic prices have continued to surge. This surge prompted President Tinubu in 2025 to adopt photovoltaic systems for powering the Presidential Villa and Aso Rock. Similarly, communities in rural areas without grid access now face increasing difficulties in generating electricity due to the escalating cost of fossil fuels [10]. In 2018, the Indonesian government introduced the Rooftop Photovoltaic Solar Systems (RPVSS) policy, enabling customers of the State Electricity Company to generate electricity through solar PV systems and export surplus power to the national grid at 65% of the retail tariff. This initiative aimed to increase the share of renewable energy in the national energy mix to 23% by 2025 [11]. Photovoltaic technology offers a practical solution to the rising costs of fossil fuels and the global challenges of climate change [12]. Owing to its advantages over conventional power generation systems, demand for PV continues to grow in the renewable energy market, positioning it as a key contributor to future energy sustainability [13].

Global energy demand has increased substantially from 8,588 million tonnes of oil equivalent (Mtoe) in 1995 to 13,147 Mtoe in 2015, with emerging economies such as India and China emerging as the leading consumers by Kapilan *et al.* [14]. Energy performance is a core component of energy policy and a critical enabler of sustainable global economic growth [14]. Climate change and rapid population growth are among the top global drivers of energy demand. Energy efficiency, consumer behaviour, infrastructure investment, and financial shocks influence national economies, while governance and international relations shape the global energy market. Advancements in renewable energy technologies, alongside innovations in the oil and gas sector, are significant drivers of global energy dynamics [15]. Global energy consumption is

projected to increase by up to 50% between 2005 and 2030, with developing countries such as India and China emerging as the leading consumers [16].

In Nigeria, many individuals adopt photovoltaic (PV) systems as an alternative to fossil fuel-based electricity due to rising fuel costs. However, expectations of consistent optimal performance throughout the day, months, and seasons often lead to disappointment. Users commonly assume that PV systems will deliver outputs identical to those stated in manufacturer specification sheets, which are determined under standard test conditions in controlled environments. In reality, outdoor performance is influenced by variable meteorological factors and therefore deviates from laboratory specifications [17]. Unrealistic expectations have caused some users to abandon PV systems in frustration, reverting to fossil fuel generators, while others persist with dissatisfaction. This challenge arises largely from the absence of localized performance data to guide realistic expectations. Consequently, this research seeks to provide empirical insights into the monthly performance of PV systems for electricity generation in Calabar.

With the rapid expansion of solar PV applications, understanding their operational performance has become a critical area of research. Reliable knowledge of PV output under real weather conditions is essential for system design, configuration, and product selection [18]. Similarly, engineers must evaluate PV performance in actual operating environments, as manufacturer specifications alone cannot provide accurate data for general conditions.

The performance of a PV system is influenced not only by its inherent features—such as solar cell technology, charge controller design, battery type, and inverter configuration—but also by the climatic conditions at the installation site [19]. Among these factors, solar irradiance plays a particularly significant role, as its continuous variation directly affects electricity generation. Thus, the energy output of PV systems at any given moment remains strongly dependent on prevailing climatic conditions [20].

Numerous studies exist that explore the performance of photovoltaics in various locations. Takyi and Laryea [21] compared different PV technologies in Kumasi, Ghana. The findings indicated that the degradation rates of polycrystalline PV modules in Ghana range from 1.6% to 1.75% per year, leading to total power losses of between 15% and 21%. These exceed the typical benchmark of 1% per year for 25-year warranties. A performance evaluation of various crystalline silicon photovoltaic technologies was conducted by Yu *et al.* [22] in Pingshan, China. The results indicated that the silicon heterojunction (SHJ) PV module achieved the highest energy yield, averaging approximately 6% more than monocrystalline and polycrystalline PV modules. The researchers attributed the superior performance of the SHJ module to its lower temperature coefficient (0.29%/°C compared to 0.41%/°C), which effectively minimized midday summer thermal losses—less than 10% for SHJ versus roughly 14% for traditional crystalline silicon modules. A study conducted by Khanam *et al.* [23] examined the performance efficiency of monocrystalline silicon, polycrystalline silicon, and thin-film photovoltaic (PV) modules across four distinct climatic zones in India: New Delhi, Srinagar, Bangalore, and Jodhpur. These cities were chosen to represent a range of climates—from hot and humid to high-altitude cold—allowing for an analysis of performance variations influenced by regional environmental conditions. The results demonstrated that thin-film PV modules consistently exhibited superior annual energy output compared to monocrystalline and polycrystalline modules across all four climatic zones. The researchers concluded that the selection of PV technology should be tailored to the specific climate of the location. A comparative analysis was conducted by Ma *et al.*

[24] on multi-crystalline silicon (m-Si), Heterojunction with Intrinsic Thin-layer (HIT), and Cadmium Telluride (CdTe) photovoltaic modules placed on floating platforms over water bodies. The objective was to evaluate their degradation and efficiency in aquatic environments compared to traditional land-based installations. This research was carried out at Tianjin University in China. The findings indicated that HIT modules exhibited the least degradation, with a rate of approximately 0.50% per year, closely matching their performance on land. In contrast, m-Si modules experienced a higher degradation rate of about 1.32% per year on water, surpassing the land installation rate of approximately 0.93%. CdTe modules showed a degradation rate of 1.68% per year in aquatic settings, slightly higher than the land-based degradation rate of around 1.41%. The authors determined that the selection of photovoltaic technology should consider the environmental context. For floating applications, they recommended utilizing HIT modules due to their exceptional durability and minimal degradation rates. A study conducted by Schweiger *et al.* [25] over two years across multiple sites monitored the performance of 15 different photovoltaic (PV) module technologies in four distinct climate zones: temperate Germany, the alpine region of northern Italy, hot-humid India, and hot-dry Arizona (USA). The findings revealed significant variations in degradation rates, influenced by climate and module type. Modules in hot-humid and hot-dry climates experienced more rapid performance declines than temperate and alpine environments. In Germany and the Alps, degradation rates were relatively modest, whereas in India and Arizona, the steeper declines indicated stronger effects from elevated temperatures, humidity, and irradiance stress. The study concluded that cooler climates are associated with more stable output over time, while hot and humid environments accelerate degradation—highlighting the importance of aligning PV technology with local climate resilience. Atia *et al.* [26] conducted a detailed field-based evaluation of 24 monocrystalline photovoltaic (PV) modules that had been running on rooftops in Cairo, Egypt for 25 years. The study aimed to evaluate long-term degradation by analyzing variations in electrical performance parameters and energy yield over time. The results demonstrated a 23.3% decline in the maximum power ( $P_{\max}$ ) of the modules. Additionally, the maximum voltage ( $V_{\max}$ ) and maximum current ( $I_{\max}$ ) experienced degradation of 12.16% and 7.2%, respectively. The open-circuit voltage and short-circuit current ( $I_{sc}$ ) showed degradation of 2.28% and 12.16%, respectively. Furthermore, the fill factor (FF) and performance ratio (PR) diminished by 15.3% and 85.9%, respectively.

A three-year field study was conducted by Femin *et al.* [27] to evaluate the performance of six photovoltaic (PV) technologies in a tropical environment. The technologies assessed included monocrystalline silicon, polycrystalline silicon, amorphous silicon, copper indium selenium (CIS), heterojunction intrinsic thin-layer, and microcrystalline silicon. The findings indicated that the CIS technology achieved the highest annual energy output, with a performance ratio of 86.1%. In contrast, monocrystalline silicon technology experienced the most significant temperature-related energy loss, approximately 14.4%. A study by Islam *et al.* [28] examined the long-term electrical performance and ageing of field-deployed photovoltaic (PV) modules in the tropical climate of Malaysia. The research focused on modules operational for 8 years at Universiti Malaysia Pahang Al-Sultan Abdullah (UMPSA) and 10 years at Pasir Mas. The findings indicated that the average annual degradation rates at UMPSA were 0.3% for open-circuit voltage, 0.23% for short-circuit current ( $I_{sc}$ ), 0.81% for maximum power output ( $P_{\max}$ ), and 0.35% for fill factor (FF). In contrast, at Pasir Mas, the average annual degradation rates were 1.124% for  $V_{oc}$ , 0.166% for  $I_{sc}$ , 1.276% for  $P_{\max}$ , and 0.43% for

FF. Additionally, the study revealed that monocrystalline silicon modules experienced an average power degradation of 6.48%, whereas polycrystalline silicon modules faced a higher degradation of 12.76%. A study by Adouane *et al.* [29] examined the performance of eight photovoltaic (PV) technologies in Kuwait's harsh desert climate, characterized by high irradiance, extreme temperatures, and significant dust accumulation. The experiments were conducted on a raised test facility (3 meters above ground) at the Kuwait Institute for Scientific Research (KISR), near the seashore, over 12 months. The results indicated that monocrystalline, polycrystalline, and HIT PV modules performed exceptionally well under intense sunlight but experienced a rapid decline in efficiency under low irradiance conditions. In contrast, the cylindrical copper indium gallium diselenide (CIGS) module performed relatively better at low light levels. Akonjom and Njok [30] conducted an experimental evaluation to determine how key meteorological factors, such as relative humidity, panel temperature and irradiance, affect the electrical performance of photovoltaic (PV) modules in the Guinea Savannah climate of Ogoja, Nigeria. The findings indicated that voltage output remains stable when relative humidity is between 47% and 67%. However, when relative humidity falls below 47%, the voltage output becomes erratic, hindering the module's ability to reach its full efficiency. Additionally, the average panel temperature rarely exceeds 40°C, except during January, suggesting that PV modules in this location can achieve an efficiency of approximately 90%. Njok *et al.* [31] explored the influence of solar irradiance (plane-of-array) and variations in solar flux on the efficiency of polycrystalline photovoltaic (PV) modules installed near a river. The authors found that proximity to water bodies can impact module performance due to enhanced reflection, increased diffuse irradiance, and microclimatic factors, including humidity and temperature fluctuations. The results indicated that both solar flux intensity and river-related environmental conditions significantly affected energy yield and overall module efficiency. This research underscores the necessity of considering site-specific ecological factors, particularly in riverine areas, when designing and deploying PV systems.

Several studies have examined the performance of photovoltaic systems under varying climatic conditions; however, much of the available data remains region-specific. There is limited information on the monthly variations in the output electrical performance of polycrystalline photovoltaic modules for household applications in Calabar, which is essential for effective system design and sizing [32]. While different PV modules and systems have been investigated across diverse climatic and geographical settings, this study considers solar irradiance, month of the year, and time of day.

Manufacturer specifications of PV modules often deviate from actual outdoor performance, making it necessary to account for local climatic conditions at the installation site [33, 34]. In southern Cross River State, Nigeria, limited research exists on the monthly variations in the electrical output of polycrystalline PV systems for household applications, particularly concerning manufacturer specifications. In practice, system monitoring after installation is challenging, yet climatic factors strongly influence performance at any given time. To address this gap, monthly performance analyses have been undertaken [35, 36]. Without knowledge of seasonal efficiency patterns, users may experience unmet expectations. This study provides insights to help identify the monthly performance of PV systems.

Throughout this paper, “solar irradiance” denotes the optical input at the module plane, expressed as power per area ( $\text{W m}^{-2}$ ) and measured by the irradiance meter; it is the independent driver for performance plots and thresholds (*e.g.*,  $\approx 200$  and  $>1000$  W

$\text{m}^{-2}$ ). “PV output power” denotes the electrical response of the module (W), computed from the measured current and voltage at the maximum power point. This distinction avoids conflating the optical resource with the electrical output and ensures unit consistency in figures and equations, where H represents incident irradiance.

## Materials and Methods

This section outlines the materials employed in the study, the setup configuration, and the procedures adopted for measurement and data acquisition.

### Materials Employed in the Study

The study utilized a polycrystalline photovoltaic module (model: AF-130W) manufactured by Africell Solar, with a rated maximum power of 130 W. The module’s output electrical characteristics are shown in Table 1. A high-precision digital maximum power point (MPP) tracker (model: WS400A) was employed to measure and record the maximum power, voltage, and current generated by the module. In addition, a digital solar irradiance (plane-of-array) meter (model: SM206) was used to monitor and ascertain the solar irradiance incident on the PV module surface.

**Table 1.** PV Module Technical/Electrical Characteristics

Electrical Specification	Value
Maximum Power	130 W
Current at Maximum Power	7.18 A
Voltage at Maximum Power	18.10 V
Short Circuit Current	7.91 A
Open-circuit Voltage	21.72 V
Number of cells	36
Module dimension	1480mm*670mm*35mm
Model	AF-130 zW
Manufacturer	Africell Solar

### Experimental Setup

The PV module was installed horizontally with its surface facing the sun on a platform one metre above ground level, as shown in Fig. 1. Output cables from the module were connected to a two-way switch. One output of the switch was linked to the MPP tracker to monitor maximum power points (Fig. 2), while the other was connected to the input of a solar charge controller. The controller’s output was directed to a solar gel battery to facilitate stable charging, and the stored energy was subsequently used to power loads through an inverter.

### Measurement Procedure

Measurements were conducted over three months, from July to September, at 30-minute intervals between 06:00 and 18:00. During the data collection, the time of day was also recorded. The output power, current, and voltage from the PV module were measured using an intelligent maximum power point (MPP) tracker. The solar irradiance



**Figure 1.** Photovoltaic module on a platform 1 metre high

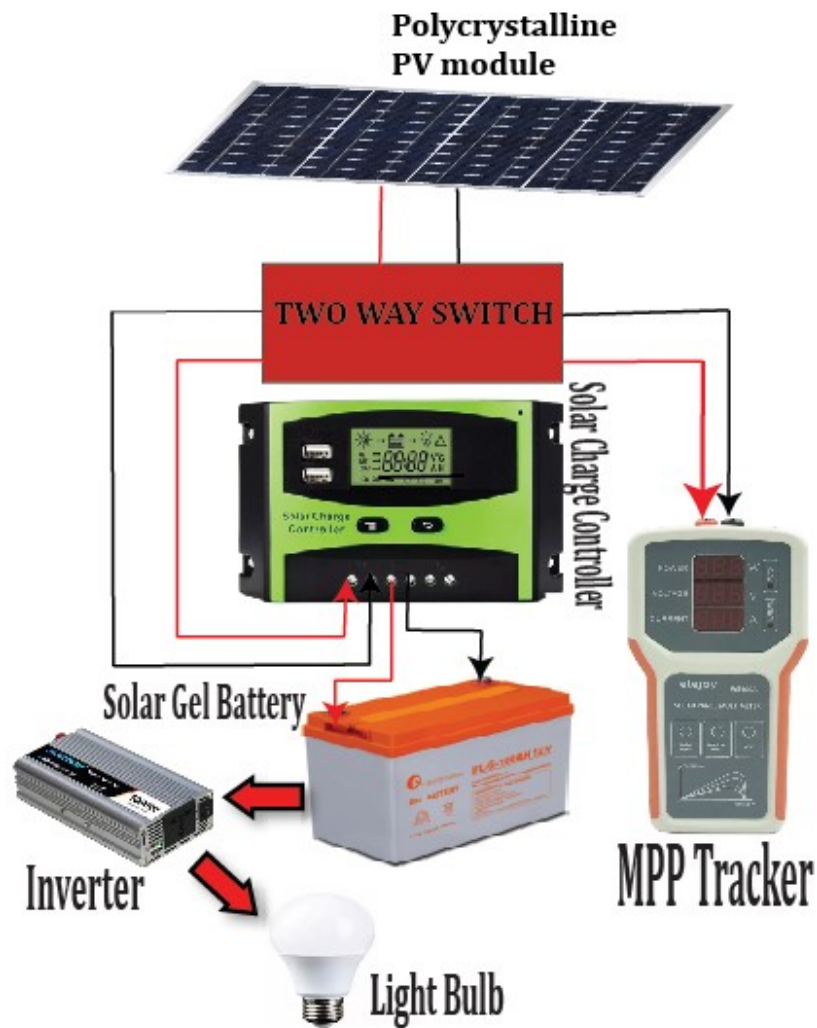


**Figure 2.** The Experimental Setup

(plane-of-array) level at the surface of the PV technology was measured via the digital solar irradiance (plane-of-array) meter.

The optical input used in this study is plane-of-array irradiance, expressed in  $\text{W m}^{-2}$ . Irradiance was measured at the module surface using a digital solar power meter (SM206) positioned co-planar with the PV module and sampled every 30 minutes in tandem with MPP-tracker electrical readings ( $V_{MP}I_{MP}P_{MP}$ ). Throughout the manuscript this quantity is denoted as  $G_{POA}$  (also  $H$  in the governing equations) and represents the instantaneous radiant power per unit area incident on the module. Electrical output (power in W, energy in Wh/kWh) is reported separately.

### Data Processing

In this study, the phrase “solar irradiance (plane-of-array)” ( $\text{W m}^{-2}$ ) refers to plane-of-array solar irradiance—the instantaneous radiant power per unit area incident on the module surface (hereafter irradiance,  $G_{POA}$ ). Electrical quantities from the PV module are denoted separately: output power  $P_{out} = V_{MP}I_{MP}$  in watts (W), energy in watt-hours (Wh) or kilowatt-hours (kWh), current (A), and voltage (V). Unless otherwise stated, thresholds reported as “ $200 \text{ W m}^{-2}$ ” or “ $>1000 \text{ W m}^{-2}$ ” pertain to irradiance at the module plane, measured by the hand-held irradiance meter.  $H$  in the equations denotes incident irradiance ( $\text{W m}^{-2}$ ). The study was conducted under real outdoor conditions with fluctuating solar irradiance (plane-of-array). The instantaneous voltage ( $V_{MP}$ ), current ( $I_{MP}$ ), and maximum power ( $P_{MP}$ ) at maximum power, at specific solar irradiance (plane-of-array) levels, were measured directly using the intelligent PV module MPP tracker. The efficiency of a PV system is strongly influenced by its voltage and current output, which are in turn affected by climatic factors such as solar irradiance (plane-of-array) and maintenance. Both the current at maximum power ( $I_{MP}$ ) and the voltage at maximum power ( $V_{MP}$ ) are significantly determined by system design, maintenance practices, and solar irradiance (plane-of-array) ( $H$ ), as expressed in equations (1) and (2) [37].

#### Load Current:

$$I_{MP} = I_{PH} - I_0 \left[ e^{\frac{qV_{MP}}{K_B T}} - 1 \right] \quad (1)$$

#### Load Voltage:

$$V_{MP} = \frac{K_B T}{q} \ln \left[ \frac{I_{PH} + I_0 - I_{MP}}{I_0} \right] \quad (2)$$

#### Short Circuit Current:

$$I_{PH} = I_{SC} = bH \quad (3)$$

where  $I_{PH}$  is the photogenerated current, which is the short circuit current  $I_{SC}$  as expressed in equation (3) also by [37].  $b$  is a constant that is determined by the junction properties of the semiconductor, and  $H$  is the incident solar irradiance (plane-of-array) reaching the PV module.  $I_0$  is the diode reverse saturated current,  $K_B$  is the Boltzmann constant,  $T$  is the absolute temperature,  $q$  is the electronic charge, and  $e$  is the exponential symbol. From the data obtained, the dynamic efficiency of the PV modules was computed with (4), while the PV module efficiency at standard test conditions [1] was confirmed via (5) as shown by [37].

#### Dynamic Efficiency:

$$\eta_P = \frac{P_{MEA}}{P_{MAX}} \times 100\% \quad (4)$$

where  $P_{MEA}$  and  $P_{MAX}$  are the measured power and the maximum power of the PV module at STC respectively.

Module efficiency at standard test conditions (STC: 1000 W m<sup>-2</sup>, 25°C cell temperature, AM 1.5G spectrum) was confirmed via (5):

$$\eta_{MOD} = \frac{\text{Power of photovoltaic module} \times 100\%}{\text{Area of photovoltaic module} \times 1000 \text{ W/m}^2} \quad (5)$$

## Study Area

The study was conducted in Calabar, the capital of Cross River State in southern Nigeria, located at 4°57'06" N latitude and 8°19'19" E longitude, with an elevation of 32 meters above sea level. The region is characterised by a tropical monsoon climate, marked by heavy rainfall for most of the year and two short dry seasons, typically from January to March and October to December [37]. Overall, Calabar remains hot and humid year-round, with overcast conditions prevailing during the wet season and predominantly cloudy skies during the dry season. Sunshine duration also varies seasonally, with December recording the highest average of 9.5 hours per day, while August receives the lowest, at approximately 4 hours daily [38].

## Results and Discussion

This section explains data from in-situ measurements and analysis, structured into two parts. The first part examines the monthly fluctuations in the level of solar irradiance (plane-of-array) diurnally, as illustrated in Fig. 3. The second part provides an analysis of the results, focusing on the monthly output electrical performance of the PV module with varying solar irradiance (plane-of-array), as shown in Fig. 4.

Table 2 displays the monthly descriptive analysis of the amount of solar irradiance (plane-of-array) reaching the PV module surface. Tables 3, 4 and 5 show the monthly descriptive analysis of the output electrical parameters from the PV module.

It is pertinent to understand that the output electrical parameters ( $V_{MP}$ ,  $I_{MP}$ ,  $P_{MP}$ , and  $\eta_P$ ) used in the analysis of the results are the maximum voltage, current, power, and efficiency, respectively, that the PV module produces instantly under a particular level of solar irradiance (plane-of-array) (atmospheric condition).

**Table 2.** Descriptive analysis of monthly plane-of-array irradiance,  $G_{POA}$  (W m<sup>-2</sup>) at PV modules surface

Statistics	Solar irradiance (plane-of-array) (W/m <sup>2</sup> )	Solar irradiance (plane-of-array) (W/m <sup>2</sup> )	Solar irradiance (plane-of-array) (W/m <sup>2</sup> )
Month	July	August	September
Minimum	0	0	0
Maximum	930.3	625.9	783.5
Range	930.3	625.9	783.5
Mean	301.7	274.7	328.8
Median	300	259.4	299.2
Variance	57000.4	38090.3	60775.4
Standard Deviation	238.8	195.2	246.5
Standard Error	47.8	39	49.3

Descriptive statistics of plane-of-array irradiance,  $G_{POA}$  ( $\text{W m}^{-2}$ ) measured on the PV module surface with a digital solar power meter (SM206). Values are the instantaneous irradiance readings taken at 30-minute intervals (06:00–18:00) during July–September, concurrent with electrical measurements from the MPP tracker.

**Table 3.** Descriptive analysis of output electrical parameters from PV module in July

Statistics	$V_{MP}$ (V)	$I_{MP}$ (A)	$P_{MP}$ (W)	$\eta_P$ (%)
Minimum	0.79	0	0	0%
Maximum	18.46	6.14	112.57	87%
Range	17.67	6.14	112.57	87%
Mean	16.81	1.97	36.92	28%
Median	18.04	1.9	41.23	32%
Variance	15.63	2.46	824.52	5%
Standard Deviation	3.95	1.57	28.71	22%
Standard Error	0.86	0.33	5.99	5%

**Table 4.** Descriptive analysis of output electrical parameters from PV module in August

Statistics	$V_{MP}$ (V)	$I_{MP}$ (A)	$P_{MP}$ (W)	$\eta_P$ (%)
Minimum	2.4	0	0	0%
Maximum	18.4	4.44	82.36	63%
Range	16	4.44	82.36	63%
Mean	16.3	1.91	34.66	27%
Median	18.04	1.89	34.6	27%
Variance	17.71	1.92	652.18	4%
Standard Deviation	4.21	1.39	25.54	20%
Standard Error	1.09	0.29	5.32	4%

**Table 5.** Descriptive analysis of output electrical parameters from PV module in September

Statistics	$V_{MP}$ (V)	$I_{MP}$ (A)	$P_{MP}$ (W)	$\eta_P$ (%)
Minimum	2.43	0	0	0%
Maximum	18.35	5.05	92.02	71%
Range	15.92	5.05	92.02	71%
Mean	16.71	2.17	41.23	32%
Median	18.03	2.11	39.23	30%
Variance	15.05	2.98	948.8	6%
Standard Deviation	3.88	1.73	30.8	24%
Standard Error	0.94	0.37	6.29	5%

#### Diurnal and Monthly Variations in the Level of Solar Irradiance (plane-of-array)

Figure 3 shows how the level of solar irradiance (plane-of-array) varies daily for each month. The figure reveals an almost linear increase in solar irradiance (plane-of-array) between 06:00 and 12:00. Also, the figure reveals peaks in the level of solar irradiance (plane-of-array). These are periods when solar irradiance (plane-of-array) is at its highest. In July, the peak in solar irradiance (plane-of-array) is observed at 12:00. In August, the peak is observed at 12:30. In September, double peaks in solar irradiance (plane-of-array) are at 11:00 and 14:00.

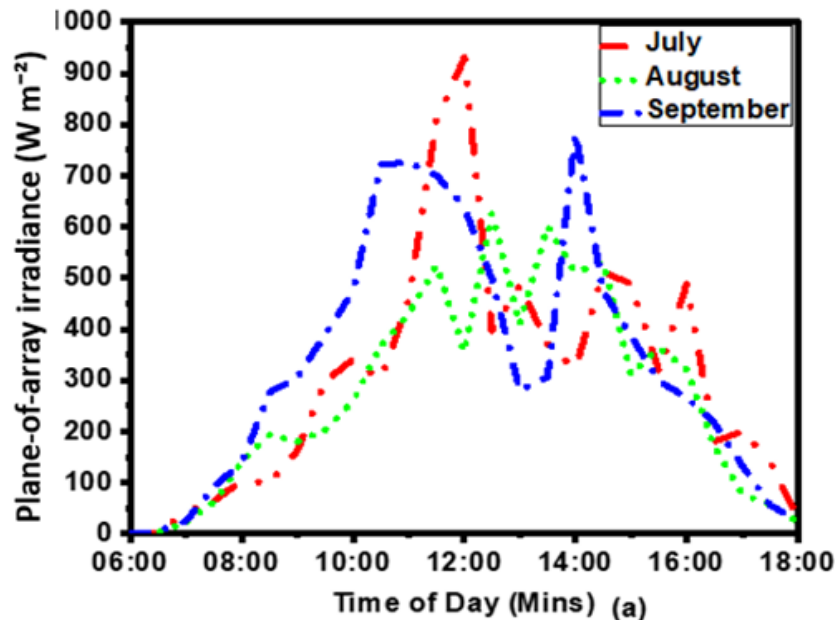


**Figure 3.** Daily energy variations in solar irradiance levels (plane-of-array).

#### Monthly Performance in PV Module Output Electrical Parameters under Varying Solar Irradiance (plane-of-array)

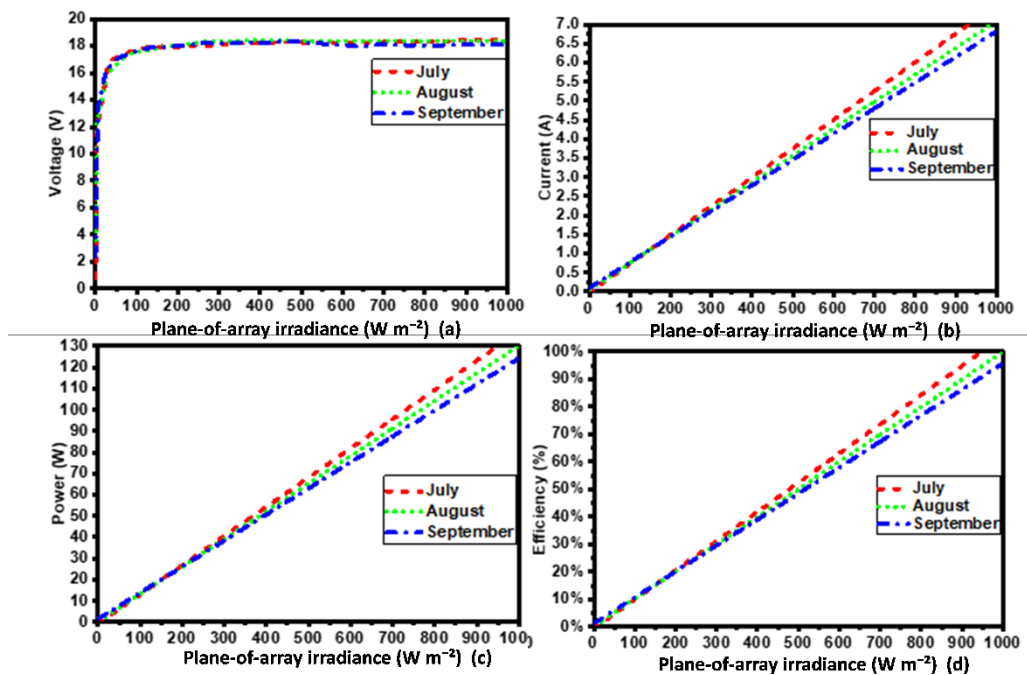
Figure 4a depicts the monthly voltage performance from the PV module with solar irradiance (plane-of-array). The figure reveals some interesting trends as it shows that, regardless of the month, voltage increases between 0 and 200  $\text{W}/\text{m}^2$  of solar irradiance (plane-of-array) before attaining stability close to the voltage at STC, which agrees with earlier studies by [31]. Still, in Figure 3, a slight ripple trend is visible as solar irradiance (plane-of-array) increases. This ripple as solar irradiance (plane-of-array) increases is due to the fluctuations in panel temperature with varying solar irradiance (plane-of-array), which conforms to earlier studies by [34], which reveal that about 0.5 V is lost or gained for every degree rise or drop in temperature, respectively. Furthermore, the figure demonstrates that harvesting maximum voltage from a polycrystalline PV module is possible regardless of the month as long as the solar irradiance (plane-of-array) level does not drop below 200  $\text{W}/\text{m}^2$ .

Figure 4b portrays the monthly output-current performance from the PV module with solar irradiance (plane-of-array). The figure shows that regardless of the month, a linear positive trend is observed as solar irradiance (plane-of-array) increases, confirming that a linear relationship exists between solar irradiance (plane-of-array) and current, which also agrees with earlier work by [31]. The figure interestingly reveals the PV module having the highest output-current performance in July, and the least performance in September, despite August having the fewest sunshine hours. Furthermore, Figure 3 shows that harvesting maximum current from the PV module, as specified in the manufacturer's technical data (Table 1), is possible in July. In August and September, harvesting maximum current from the PV module will be difficult because the level of solar irradiance (plane-of-array) at the module surface has to be in excess of 1000  $\text{W}/\text{m}^2$ .

Figure 4c illustrates the monthly output power performance of the PV module as a function of solar irradiance (plane-of-array). The results indicate that, irrespective of the

month, the output power exhibits a linear positive trend with increasing solar irradiance (plane-of-array), consistent with the findings of [37], which confirm the existence of a linear relationship between solar irradiance (plane-of-array) and PV output power. Notably, the module demonstrates its highest output performance in July and its lowest in September, despite August recording the fewest sunshine hours. Furthermore, Figure 3 highlights that achieving the maximum power output specified in the manufacturer's technical data (Table 1) is unattainable in September, as the incident solar irradiance (plane-of-array) on the module surface would need to exceed  $1000 \text{ W/m}^2$ . A closer inspection of the figure reveals that the module delivers approximately the same output power within the solar irradiance (plane-of-array) range of  $0$  to  $450 \text{ W/m}^2$ , regardless of the month.

Figure 4d unravels how efficient the PV module is monthly as solar irradiance (plane-of-array) varies. The figure reveals that between  $0$  and  $400 \text{ W/m}^2$ , the monthly PV module efficiency is the same regardless of the month. Above  $400 \text{ W/m}^2$ , the module is most efficient in July and least efficient in September. Interestingly, the PV module is more efficient in August than in September despite August having fewer sunshine hours. Furthermore, Figure 4d highlights that achieving  $100\%$  efficiency from the PV module is unattainable in September, as the incident solar irradiance (plane-of-array) on the module surface would need to exceed  $1000 \text{ W/m}^2$ , even though September has more sunshine hours than August.



**Figure 4.** Monthly variations in PV module output electrical parameters under varying incident solar power (plane-of-array)

### Implications of the Study for Household Use in Calabar

The results of this study hold significant implications for household energy security in Calabar, particularly in the era of sustainable development and the global net-zero agenda. Localized performance data on monthly photovoltaic (PV) variability provide households with realistic expectations, reducing the reliance on generic

manufacturer specifications that often misrepresent actual field conditions. Such context-specific insights are crucial for boosting public confidence in PV technology and stimulating greater adoption, consistent with [39] emphasis on advancing applied energy solutions to address regional energy access challenges.

From the perspective of global decarbonization efforts, these findings reinforce the role of PV systems as a critical enabler of Nigeria's net-zero transition. Distributed solar energy has been identified by the International Energy Agency [40] as central to achieving emission reduction targets. The demonstrated ability of polycrystalline PV modules to deliver meaningful energy outputs even during low-sunshine months implies that households can incrementally replace fossil fuel generators. This household-level shift aligns directly with broader climate action objectives, advancing low-carbon energy pathways while reducing environmental and health impacts associated with fossil fuel use.

At the household system design level, the study provides empirical guidance for optimizing PV configurations, storage, and load management. Okonkwo *et al.* [41] showed that environmental variability exerts a strong influence on PV output, and the observed challenges in achieving peak power in September validate the importance of climate-responsive system sizing. Households can better calibrate battery capacity and inverter specifications using such data, enhancing operational efficiency and minimizing losses. This strengthens the resilience of household energy systems and aligns with the sustainable development goal (SDG) of ensuring access to affordable and clean energy.

The findings also highlight the necessity for climate-resilient infrastructure planning. Obiwulu *et al.* [42] emphasized that variability and intermittency must be considered in renewable energy system integration. In Calabar's tropical and humid environment, monthly performance data enable households to design hybrid systems that may combine PV with complementary clean technologies, such as hydrogen-based energy carriers [43]. Such hybridization ensures a stable energy supply [44], mitigates seasonal shortfalls [45], and supports the creation of adaptive energy infrastructures consistent with long-term sustainable development strategies [46].

Socio-economic implications are equally relevant. Household-level adoption of PV systems, as noted by Nwokolo *et al.* [47], contributes not only to emission reductions but also to financial savings and improved energy independence. By accounting for monthly variability in output, households can anticipate fluctuations in electricity availability, plan expenditures more accurately, and reduce frustrations stemming from unrealistic expectations. This improves household satisfaction and supports the wider social acceptance of PV technologies as a reliable [48] and cost-effective energy solution [49].

The study also provides empirical justification for technological and policy innovation. Nwokolo *et al.* [50] stressed the importance of contextualizing PV deployment within climatic realities. Policymakers in Cross River State can use these results to design incentive frameworks for residential PV adoption [51], including subsidies or tax credits [52], while promoting adaptive technologies such as automated maximum power point tracking (MPPT) systems. These approaches ensure households extract maximum value from their installations and align with Nigeria's commitments under the Paris Agreement [53].

Ultimately, the household-level implications of this study support multiple SDGs, particularly SDG 7 (Affordable and Clean Energy), SDG 11 (Sustainable Cities and Communities), and SDG 13 (Climate Action). Nwokolo *et al.* [54] argue that sustainable energy transitions require not just technological deployment but also reliable datasets that

reflect local performance realities. By filling a critical knowledge gap in Calabar, this study empowers households to actively participate in the clean energy transition. In doing so, it ensures that the renewable energy agenda is inclusive [55], equitable [56], and sustainable, positioning households as active contributors to the net-zero future [57].

## CONCLUSIONS

This study delivers a field-resolved picture of a domestic polycrystalline PV module operating in Calabar, Nigeria, using co-measured plane-of-array irradiance and MPP electrical variables every 30 minutes (06:00–18:00) across July–September. The protocol couples a digital irradiance meter with an intelligent MPP tracker on an AF-130W module, establishing a clean separation between the optical input (irradiance,  $\text{W m}^{-2}$ ) and the electrical response (V, A, W, Wh) used in all analyses.

Three quantitative operating thresholds and patterns emerge for Calabar’s monsoonal context. First, voltage stabilizes near its STC level once irradiance reaches  $\approx 200 \text{ W m}^{-2}$ , irrespective of month—an actionable signal for inverter voltage-window planning. Second, approaching manufacturer-level current (and maximum power) in August–September generally requires  $>1000 \text{ W m}^{-2}$ , a level seldom attained in those wetter months, which explains recurrent current-limited behaviour. Third, monthly performance is asymmetric: output current and power peak in July and are lowest in September, even though average monthly irradiance is highest in September and lowest in August—a counter-intuitive pattern that cautions against using sunshine duration or monthly mean irradiance as proxies for deliverable output.

Two design heuristics follow directly for household PV in Calabar. (i) Treat 0–450  $\text{W m}^{-2}$  as a conservative “uniform-power” operating band (similar output across months), and plan daytime appliances/battery charging around this plateau; performance dispersion grows beyond this band. (ii) Expect month-dependent efficiency above  $\sim 400 \text{ W m}^{-2}$  (July > August > September) and do not size systems assuming September can reach nameplate  $P_{max}$  without exceptionally high irradiance. These heuristics reduce sizing uncertainty, improve charge-controller and storage setpoints for the wet season, and align household expectations with realistic field behaviour.

Finally, these findings are location-specific contributions rather than generic theory: (a) thresholds that reconcile STC ratings with Calabar’s climate ( $\approx 200 \text{ W m}^{-2}$  voltage plateau;  $>1000 \text{ W m}^{-2}$  typically needed to approach rated current in Aug–Sep); (b) a documented seasonal inversion where September’s higher mean irradiance coincides with lower electrical output; and (c) ready-to-use planning rules (uniform-power band; efficiency ordering and September limit) for household designers. Future work should extend this co-measurement protocol to the dry season and alternative tilts/thermal co-measurements to refine current-vs-irradiance thresholds and seasonal envelopes for Calabar.

## CONFLICTS OF INTEREST

The authors declare that there is no conflict of interests regarding the publication of this paper.

## ACKNOWLEDGMENTS

The authors of this article give special thanks to Tertiary Education Trust fund (TETFund) for funding this institution-based research.

## REFERENCES

- [1] Charfi, W., Chaabane, M., Mhiri, H., & Bournot, P. (2018). Performance evaluation of a solar photovoltaic system. *Energy Reports*, 4, 400-406. doi:<https://doi.org/10.1016/j.egy.2018.06.004>
- [2] Njok, A. O., Akonjom, N. A., & Ogbulezie, J. C. (2022). Design and performance evaluation of photovoltaic systems with automatic dust wiper in a natural dusty environment. *Asian J. Phys. Chem. Sci*, 10(4), 1-15. doi:<https://doi.org/10.9734/AJOPACS/2022/v10i4186>
- [3] Andrea, Y., Pogrebnaya, T., & Kichonge, B. (2019). Effect of Industrial Dust Deposition on Photovoltaic Module Performance: Experimental Measurements in the Tropical Region. *International Journal of Photoenergy*, 2019(1), 1892148. doi:<https://doi.org/10.1155/2019/1892148>
- [4] Peng, J., Lu, L., & Yang, H. (2013). Review on life cycle assessment of energy payback and greenhouse gas emission of solar photovoltaic systems. *Renewable and Sustainable Energy Reviews*, 19, 255-274. doi:<https://doi.org/10.1016/j.rser.2012.11.035>
- [5] Tyagi, V. V., Rahim, N. A. A., Rahim, N. A., & Selvaraj, J. A. L. (2013). Progress in solar PV technology: Research and achievement. *Renewable and Sustainable Energy Reviews*, 20, 443-461. doi:<https://doi.org/10.1016/j.rser.2012.09.028>
- [6] Kim, H., Park, E., Kwon, S. J., Ohm, J. Y., & Chang, H. J. (2014). An integrated adoption model of solar energy technologies in South Korea. *Renewable Energy*, 66, 523-531. doi:<https://doi.org/10.1016/j.renene.2013.12.022>
- [7] Sampaio, P. G. V., & González, M. O. A. (2017). Photovoltaic solar energy: Conceptual framework. *Renewable and Sustainable Energy Reviews*, 74, 590-601. doi:<https://doi.org/10.1016/j.rser.2017.02.081>
- [8] Njok, A. O., Archibong, E. A., & Fischer, G. A. (2023). Diurnal analysis of the performance of photovoltaic systems under the Guinea Savannah Atmosphere in Ogoja, Cross River State, Nigeria. *Physical Science International journal*, 27(1), 1-15. doi:<https://doi.org/10.9734/PSIJ/2023/v27i176>
- [9] Nerlinger, M., & Utz, S. (2022). The impact of the Russia-Ukraine conflict on energy firms: A capital market perspective. *Finance Research Letters*, 50, 103243. doi:<https://doi.org/10.1016/j.frl.2022.103243>
- [10] Steffen, B., & Patt, A. (2022). A historical turning point? Early evidence on how the Russia-Ukraine war changes public support for clean energy policies. *Energy Research & Social Science*, 91, 102758. doi:<https://doi.org/10.1016/j.erss.2022.102758>
- [11] Setyawati, D. (2020). Analysis of perceptions towards the rooftop photovoltaic solar system policy in Indonesia. *Energy policy*, 144, 111569. doi:<https://doi.org/10.1016/j.enpol.2020.111569>

- [12] Njok, A. O., & Kamgba, F. A. (2023). Monocrystalline Photovoltaic Panel Response Pattern to Relative Humidity and Temperature under Distinct Wavelengths in Mangrove Swamp Environment in Calabar, Cross River States, Nigeria. *Journal of Applied Sciences and Environmental Management*, 27(8), 1825-1837. doi:<https://doi.org/10.4314/jasem.v27i8.29>
- [13] Khan, M. A., Ko, B., Alois Nyari, E., Park, S. E., & Kim, H. J. (2017). Performance evaluation of photovoltaic solar system with different cooling methods and a bi-reflector PV system (BRPVS): an experimental study and comparative analysis. *Energies*, 10(6), 826. doi:<https://doi.org/10.3390/en10060826>
- [14] Kapilan, N., Nithin, K. C., & Chiranth, K. N. (2022). Challenges and opportunities in solar photovoltaic system. *Materials Today: Proceedings*, 62, 3538-3543. doi:<https://doi.org/10.1016/j.matpr.2022.04.390>
- [15] Abed, K. A., El Morsi, A. K., Sayed, M. M., Shaib, A. A. E., & Gad, M. S. (2018). Effect of waste cooking-oil biodiesel on performance and exhaust emissions of a diesel engine. *Egyptian journal of petroleum*, 27(4), 985-989. doi:<https://doi.org/10.1016/j.ejpe.2018.02.008>
- [16] Li, Z., Yang, J., & Dezfuli, P. A. N. (2021). Study on the Influence of Light Intensity on the Performance of Solar Cell. *2021*(1), 6648739. doi:<https://doi.org/10.1155/2021/6648739>
- [17] Ma, T., Yang, H., & Lu, L. (2014). Solar photovoltaic system modeling and performance prediction. *Renewable and Sustainable Energy Reviews*, 36, 304-315. doi:<https://doi.org/10.1016/j.rser.2014.04.057>
- [18] Ishaque, K., & Salam, Z. (2011). An improved modeling method to determine the model parameters of photovoltaic (PV) modules using differential evolution (DE). *Solar Energy*, 85(9), 2349-2359. doi:<https://doi.org/10.1016/j.solener.2011.06.025>
- [19] Siddiqui, R., & Bajpai, U. (2012). Deviation in the Performance of Solar Module Under Climatic Parameter as Ambient Temperature and Wind Velocity in Composite Climate. *International Journal Of Renewable Energy Research*, 2(3), 486-490.
- [20] Njok, A. O., Ogbulezie, J. C., & Akonjom, N. A. (2022). Evaluation of the performance of photovoltaic system under different wavelengths from artificial light in a controlled environment. *Journal of Applied Sciences and Environmental Management*, 26(6), 1015-1020. doi:<https://dx.doi.org/10.4314/jasem.v26i6.4>
- [21] Takyi, G., & Laryea, O. G. (2021). Comparative study of the performance of solar photovoltaic module technologies installed in Kumasi, Ghana, in Sub-Saharan Africa. *Scientific African*, 13, e00877. doi:<https://doi.org/10.1016/j.sciaf.2021.e00877>
- [22] Yu, C., Chai, J., Han, S., Liu, Z., Li, X., & Yao, J. (2019). Field performance evaluation of various crystalline silicon photovoltaic technologies in Pingshan, China. *Energy Reports*, 5, 525-528. doi:<https://doi.org/10.1016/j.egyr.2019.04.006>
- [23] Khanam, S., Meraj, M., Azhar, M., Karimi, M. N., Ahmad, T., Arif, M. R., & Al-Kouz, W. (2021). Comparative performance analysis of photovoltaic modules of different materials for four different climatic zone of India. *Urban Climate*, 39, 100957. doi:<https://doi.org/10.1016/j.uclim.2021.100957>
- [24] Ma, C., Wu, R., Liu, Z., & Li, X. (2024). Performance assessment of different photovoltaic module technologies in floating photovoltaic power plants under waters environment. *Renewable Energy*, 222, 119890.

- doi:<https://doi.org/10.1016/j.renene.2023.119890>
- [25] Schweiger, M., Bonilla, J., Herrmann, W., Gerber, A., & Rau, U. (2017). Performance stability of photovoltaic modules in different climates. *25*(12), 968-981. doi:<https://doi.org/10.1002/pip.2904>
- [26] Atia, D. M., Hassan, A. A., El-Madany, H. T., Eliwa, A. Y., & Zahran, M. B. (2023). Degradation and energy performance evaluation of mono-crystalline photovoltaic modules in Egypt. *Scientific Reports*, *13*(1), 13066. doi:<https://doi.org/10.1038/s41598-023-40168-8>
- [27] Femin, V., Veena, R., Petra, M. I., & Mathew, S. (2025). Comparative analysis of different PV technologies under the tropical environments. *Scientific Reports*, *15*(1), 16371. doi:<https://doi.org/10.1038/s41598-025-99958-x>
- [28] Islam, M. I., Bin Jadin, M. S., Al Mansur, A., & Alharbi, T. (2024). Electrical Performance and Degradation Analysis of Field-Aged PV Modules in Tropical Climates: A Comparative Experimental Study. *Energy Conversion and Management: X*, *24*, 100719. doi:<https://doi.org/10.1016/j.ecmx.2024.100719>
- [29] Adouane, M., Al-Qattan, A., Alabdulrazzaq, B., & Fakhraldeen, A. (2020). Comparative performance evaluation of different photovoltaic modules technologies under Kuwait harsh climatic conditions. *Energy Reports*, *6*, 2689-2696. doi:<https://doi.org/10.1016/j.egyr.2020.09.034>
- [30] Akonjom, N. A., & Njok, A. O. (2022). Effect of Meteorological Parameters on the Performance of Photovoltaics Installed under the Guinea Savannah Atmosphere in Ogoja, Cross Rivers State, Nigeria. *Journal of Applied Sciences and Environmental Management*, *26*(7), 1299-1306. doi:<https://doi.org/10.4314/jasem.v26i7.17>
- [31] Njok, A. O., Kamgba, F. A., Panjwani, M. K., & Mangi, F. H. (2020). The influence of solar power and solar flux on the efficiency of polycrystalline photovoltaics installed close to a river. *Indonesian Journal of Electrical Engineering and Computer Science*, *17*(2), 988-996. doi:<http://doi.org/10.11591/ijeecs.v17.i2.pp988-996>
- [32] Armstrong, S., & Hurley, W. G. (2010). A new methodology to optimise solar energy extraction under cloudy conditions. *Renewable Energy*, *35*(4), 780-787. doi:<https://doi.org/10.1016/j.renene.2009.10.018>
- [33] Siddiqui, R., & Bajpai, U. (2012). Statistical analysis of solar photovoltaic module output with temperature, humidity and wind velocity in composite climate. *European Journal of Scientific Research*, *80*(4), 447-456.
- [34] Kita, T., Harada, Y., & Asahi, S. (2019). The Conversion Efficiency of a Solar Cell as Determined by the Detailed Balance Model. In *Energy Conversion Efficiency of Solar Cells* (pp. 55-79). Singapore: Springer Singapore
- [35] Bashir, M. A., Ali, H. M., Khalil, S., Ali, M., & Siddiqui, A. M. (2014). Comparison of Performance Measurements of Photovoltaic Modules during Winter Months in Taxila, Pakistan. *2014*(1), 898414. doi:<https://doi.org/10.1155/2014/898414>
- [36] C Chaichan, M. T., & Kazem, H. A. (2016). Experimental analysis of solar intensity on photovoltaic in hot and humid weather conditions. *International Journal of Scientific & Engineering Research*, *7*(3), 91-96.
- [37] Njok, A., Ogbulezie, J., & Eyire, O. (2025). The Impact of External Magnetic Field on the Output Electrical Characteristics of Polycrystalline Photovoltaic

- Modules. *Asian Journal of Research and Reviews in Physics*, 9(2), 78-94. doi:<https://doi.org/10.9734/ajr2p/2025/v9i2192>
- [38] Njok, A. O., & Kamgba, F. A. (2023). Monocrystalline Photovoltaic Panel Response Pattern to Relative Humidity and Temperature under Distinct Wavelengths in Mangrove Swamp Environment in Calabar, Cross River States, Nigeria. *Journal of Applied Sciences and Environmental Management*, 27(8), 1825-1837. doi:<https://doi.org/10.4314/jasem.v27i8.29>
- [39] Hassan, M. A., Bailek, N., Bouchouicha, K., Ibrahim, A., Jamil, B., Kuriqi, A., . . . El-kenawy, E.-S. M. (2022). Evaluation of energy extraction of PV systems affected by environmental factors under real outdoor conditions. *Theoretical and Applied Climatology*, 150(1), 715-729. doi:<https://doi.org/10.1007/s00704-022-04166-6>
- [40] IEA, P. (2022). World energy outlook 2022. Paris, France: International Energy Agency (IEA). [https://uploads.iasscore.in/pdf/CAA\\_WEEK-2\\_NOVEMBER--2022.pdf](https://uploads.iasscore.in/pdf/CAA_WEEK-2_NOVEMBER--2022.pdf) (Accessed on 11/04/2025)
- [41] Okonkwo, P. C., Nwokolo, S. C., Udo, S. O., Obiwulu, A. U., Onnoghen, U. N., Alarifi, S. S., . . . Akpan, A. E. (2025). Solar PV systems under weather extremes: Case studies, classification, vulnerability assessment, and adaptation pathways. *Energy Reports*, 13, 929-959. doi:<https://doi.org/10.1016/j.egy.2024.12.067>
- [42] Obiwulu, A. U., Erusiafe, N., Olopade, M. A., & Nwokolo, S. C. (2022). Modeling and estimation of the optimal tilt angle, maximum incident solar radiation, and global radiation index of the photovoltaic system. *Heliyon*, 8(6), e09598. doi:<https://doi.org/10.1016/j.heliyon.2022.e09598>
- [43] Okonkwo, P. C., Nwokolo, S. C., Meyer, E. L., Ahia, C. C., & Mansir, I. B. (2025). Techno-economic optimization of renewable hydrogen infrastructure via AI-based dynamic pricing. *Scientific Reports*, 15(1), 31529. doi:<https://doi.org/10.1038/s41598-025-17506-z>
- [44] Okonkwo, P. C., Nwokolo, S. C., Barhoumi, E. M., Mansir, I. B., Taura, U. H., Das, B. K., . . . Kaaf, K. A. (2025). Technical and economic feasibility assessment for hybrid energy system electricity and hydrogen generation: A case study. *Global Energy Interconnection*, 8(1), 62-81. doi:<https://doi.org/10.1016/j.gloi.2025.01.001>
- [45] Okonkwo, P. C., Nwokolo, S. C., Alarifi, S. S., Ekwok, S. E., Orji, R., Udo, S. O., . . . Akpan, A. E. (2025). Bio-inspired computational intelligence metaheuristic-based optimization and sensitivity analysis approach to determine techno-economic feasibility of hydrogen refueling stations for fuel cell vehicles. *Scientific Reports*, 15(1), 12451. doi:<https://doi.org/10.1038/s41598-025-97088-y>
- [46] Alhousni, F. K., Nwokolo, S. C., Meyer, E. L., Alsenani, T. R., Alhinai, H. A., Ahia, C. C., . . . Ahmed, Y. E. (2025). Multi-scale computational fluid dynamics and machine learning integration for hydrodynamic optimization of floating photovoltaic systems. *Energy Informatics*, 8(1), 103. doi:<https://doi.org/10.1186/s42162-025-00567-9>
- [47] Nwokolo, S. C., Obiwulu, A. U., Okonkwo, P. C., Orji, R., Alsenani, T. R., Mansir, I. B., & Orji, C. (2025). Machine learning and physics-based model hybridization to assess the impact of climate change on single- and dual-axis tracking solar-concentrated photovoltaic systems. *Physics and Chemistry of the Earth, Parts A/B/C*, 138, 103881. doi:<https://doi.org/10.1016/j.pce.2025.103881>
- [48] Nwokolo, S. C., Ogbulezie, J. C., & Ushie, O. J. (2023). A multi-model ensemble-

- based CMIP6 assessment of future solar radiation and PV potential under various climate warming scenarios. *Optik*, 285, 170956.  
doi:<https://doi.org/10.1016/j.ijleo.2023.170956>
- [49] Nwokolo, S. C., & Ogbulezie, J. C. (2018). A qualitative review of empirical models for estimating diffuse solar radiation from experimental data in Africa. *Renewable and Sustainable Energy Reviews*, 92, 353-393.  
doi:<https://doi.org/10.1016/j.rser.2018.04.118>
- [50] Nwokolo, S. C., Eyime, E. E., Obiwulu, A. U., Meyer, E. L., Ahia, C. C., Ogbulezie, J. C., & Proutsos, N. (2024). A multi-model approach based on CARIMA-SARIMA-GPM for assessing the impacts of climate change on concentrated photovoltaic (CPV) potential. *Physics and Chemistry of the Earth, Parts A/B/C*, 134, 103560. doi:<https://doi.org/10.1016/j.pce.2024.103560>
- [51] Benatallah, M., Bailek, N., Bouchouicha, K., Sharifi, A., Abdel-Hadi, Y., Nwokolo, S. C., ... & M. El-kenawy, E. S. (2024). Solar Radiation Prediction in Adrar, Algeria: a Case Study of Hybrid Extreme Machine-based techniques. *International Journal of Engineering Research in Africa*, 68, 151-164.  
doi:<https://doi.org/10.4028/p-VH0u4y>
- [52] Beitelmal, W. H., Nwokolo, S. C., Meyer, E. L., & Ahia, C. C. (2024). Exploring adaptation strategies to mitigate climate threats to transportation infrastructure in Nigeria: Lagos City, as a case study. *Climate*, 12(8), 117.  
doi:<https://doi.org/10.3390/cli12080117>
- [53] Nwokolo, S. C. (2017). A comprehensive review of empirical models for estimating global solar radiation in Africa. *Renewable and Sustainable Energy Reviews*, 78, 955-995. doi:<https://doi.org/10.1016/j.rser.2017.04.101>
- [54] Nwokolo, S. C., Proutsos, N., Meyer, E. L., & Ahia, C. C. (2023). Machine learning and physics-based hybridization models for evaluation of the effects of climate change and urban expansion on photosynthetically active radiation. *Atmosphere*, 14(4), 687. doi:<https://doi.org/10.3390/atmos14040687>
- [55] Nwokolo, S. C., Meyer, E. L., & Ahia, C. C. (2023). Credible pathways to catching up with climate goals in Nigeria. *Climate*, 11(9), 196.  
doi:<https://doi.org/10.3390/cli11090196>
- [56] Nwokolo, S. C. (2025). Climate hoax: The shift from scientific discourse to speculative rhetoric in climate change conversations. *Next Research*, 2(2), 100322.  
doi:<https://doi.org/10.1016/j.nexres.2025.100322>
- [57] Okonkwo, P. C., Nwokolo, S. C., & Shammass, M. I. (2025). *Net-Zero Transit: The Future of Eco-Friendly Transportation*. Elsevier.  
doi:<https://doi.org/10.1016/C2024-0-02490-3>

**Article Copyright:** © 2025 Julie C. Ogbulezie, Samuel Chukwujindu Nwokolo and Armstrong O. Njok. This is an open access article distributed under the terms of the [Creative Commons Attribution 4.0 International License](https://creativecommons.org/licenses/by/4.0/), which permits unrestricted use and distribution provided the original author and source are credited.

